

Efficient room-temperature synthesis of crosslinked polyhydroxyurethanes from 5-membered cyclic carbonates without solvent or catalyst

P. Helbling^{1,2}, C. Desgoulières¹, F. Hermant², M. Petit², T. Vidil^{1} and H. Cramail^{1*}*

¹Univ. Bordeaux, CNRS, Bordeaux INP, LCPO, 16 avenue Pey-Berland 33600 Pessac, France

²Saint-Gobain Recherche Paris, 41 Quai Lucien Lefranc 93300 Aubervilliers, France

Table of content

I. EXPERIMENTAL SECTION	2
1. MATERIALS	2
2. CHARACTERIZATION METHODOLOGIES	2
A. INFRARED SPECTROSCOPY	2
B. RHEOMETRY	2
C. THERMOGRAVIMETRIC ANALYSIS (TGA)	3
D. DIFFERENTIAL SCANNING CALORIMETRY (DSC)	3
E. SIZE EXCLUSION CHROMATOGRAPHY (SEC)	3
F. SWELLING TESTS.....	3
G. TENSILE TESTS.....	3
3. SYNTHESIS OF AGC	4
4. SYNTHESIS TRI-5CC AND TETRA-5CC	4
5. PREPARATION OF PHU THERMOSETS	4
6. IN-SITU MONITORING OF THE PHU CROSSLINKING REACTION	4
A. INFRARED MONITORING	5
B. RHEOLOGY MONITORING	5
7. CALCULATION OF THE CONVERSION AT THE GEL POINT, A_{GEL}, ACCORDING TO THE FLORY-STOCKMAYER THEORY	5
II. SUPPLEMENTARY DATA	8
1. NMR, FTIR AND MS CHARACTERIZATIONS OF AGC	8
2. KINETICS FOR THE SYNTHESIS OF TRI-5CC AND TETRA-5CC	11
3. NMR, FTIR AND MS CHARACTERIZATIONS OF TRI-5CC	11
4. NMR, FTIR AND MS CHARACTERIZATIONS OF TETRA-5CC	13
5. FTIR SPECTRA OF P1 TO P6 (AMINE SCREENING AT RT)	15
6. SEC ANALYSIS OF THE SOLUBLE FRACTION FOR THE THERMOSETS P1 TO P6	17
7. IN-SITU FTIR MONITORING FOR THE CROSSLINKING REACTION OF P7 TO P10	17
8. IN-SITU RHEOLOGY MONITORING FOR THE CROSSLINKING REACTION OF P7 TO P10	19
9. SEC ANALYSIS OF THE SOLUBLE FRACTION FOR THE THERMOSETS P6 TO P10	22

10. DSC CHARACTERIZATION OF P8 AFTER DRYING AT 40 °C UNDER VACUUM.....	22
11. DSC CHARACTERIZATION OF THE THERMOSETS P6 TO P10	23
12. STRESS – STRAIN PROFILES FOR ALL THE TESTED SPECIMENS OF P6 TO P10.....	24
13. FTIR SPECTRA AFTER 1-MONTH STORAGE FOR P6 TO P10	26
14. DSC THERMOGRAMS AFTER 1-MONTH STORAGE FOR P6 TO P10	28
15. FTIR ANALYSIS OF THE TRI-5CC + TDA SYSTEM CROSSLINKED AT RT UNDER INERT ATMOSPHERE	29
16. SEC ANALYSIS OF THE SOL FRACTION OF THE TRI-5CC + TDA SYSTEM CROSSLINKED AT RT UNDER INERT ATMOSPHERE	30
III. REFERENCES	31

I. Experimental section

1. Materials

3-Allyloxy-1,2-propanediol is sourced from TCI Chemicals (99%), dimethyl carbonate from Fisher Scientific (99%), and triazabicyclodecene from Sigma-Aldrich (TBD, 98%). The latter is dried under vacuum prior to use. Trimethylolpropane tris(3-mercaptopropionate) (95%) and pentaerythritol tetrakis(3-mercaptopropionate) (95%) are from Sigma-Aldrich. Isophorone diamine (IPDA, 99% mixture of cis and trans) and tetraethylenepentamine (TEPA, $\geq 95\%$) are sourced from Acros Organics; 1,13-diamino-4,7,10-trioxatridecane (tDA, 98%), m-xylylene diamine (mxDA, 99%), 2-methyl-1,5-diaminopentane (2MDPA, $> 98\%$), and 1,8-octanediamine (8DA, 98%) are from TCI Chemicals; Priamine 1075 is from Croda. THF is sourced from VWR.

2. Characterization methodologies

a. Infrared spectroscopy

Fourier transform infrared (FTIR) spectra were recorded on a Bruker-VERTEX 70 instrument (400 to 4000 cm^{-1} , 4 cm^{-1} resolution, 32 scans, DLaTGS MIR) equipped with a Pike GladiATR optical design (diamond crystal) for attenuated total reflectance (ATR). In the case of *in-situ* monitoring, the spectrometer was equipped with a thermally controlled diamond plate surrounded by a metallic piece creating a leak-proof cavity in order to proceed to the crosslinking reaction directly on the plate.

b. Rheometry

Rheological monitoring of the crosslinking reactions was performed using an Anton Paar MCR 302 rheometer equipped with disposable parallel plates ($\text{Ø} = 25 \text{ mm}$) and operating in the multiwave mode using Fourier transform mechanical spectroscopy (FTMS). A multiwave strain signal of 1 % amplitude

for the 1 rad s^{-1} component was applied in order to collect G' and G'' data every 5 minutes for the 7 following frequencies: 1, 3, 6, 10, 30, 60 and 100 rad s^{-1} .

c. Thermogravimetric analysis (TGA)

The thermal decomposition of the polymer networks was studied using a TA Instruments Q50. The samples were, in a first time, heated from 20 to $600 \text{ }^\circ\text{C}$ under a nitrogen atmosphere at a rate of $10 \text{ }^\circ\text{C min}^{-1}$ and then heated until $700 \text{ }^\circ\text{C}$ under air atmosphere.

d. Differential scanning calorimetry (DSC)

Differential Scanning Calorimetry thermograms were recorded on a TA instrument DSC Q100. The samples, whose mass is comprised between 3 and 9.5 mg, were sealed in aluminium pans and analysed under nitrogen atmosphere. Two cycles were performed: a first one from $-75 \text{ }^\circ\text{C}$ to $180 \text{ }^\circ\text{C}$ at a rate of $10 \text{ }^\circ\text{C min}^{-1}$ and a second one from $-75 \text{ }^\circ\text{C}$ to $220 \text{ }^\circ\text{C}$. The glass transition temperature (T_g) was measured from the latter.

e. Size exclusion chromatography (SEC)

Polymer molar masses were determined by SEC using tetrahydrofuran (THF) as the eluent. Measurements were performed on an Ultimate 3000 system from ThermoScientific equipped with a diode array detector (DAD). A multi-angles laser light scattering detector (MALLS) and differential refractive index detector (dRI) from Wyatt technology are also included. Species were separated on three TOSOH HXL gel column G2000, G3000 et G4000 ($300 \times 7,8 \text{ mm}$, exclusion limits from 1000 Da to 400000 Da) at a flowrate of 1 mL min^{-1} . The temperature of the columns was held at $40 \text{ }^\circ\text{C}$. Easivial Polystyrene kit from Agilent was used for the standards (M_n from 162 to 364 000 Da).

f. Swelling tests

Swelling tests are carried out at room temperature in THF or deionized water. Samples with an initial mass m_0 ($\sim 0.04 \text{ g}$) are immersed in the solvent ($\sim 6 \text{ mL}$) and weighed several times a day, removing the excess solvent from their surface. The polymers are immersed until their mass stabilizes at m_s (g) over at least three measurements. The samples are then dried under vacuum at $T = 40 \text{ }^\circ\text{C}$ for 4 hours, and their mass is measured after this step to give the dry mass m_d (g). The solvent containing the soluble fraction is kept for subsequent analysis by SEC.

The swelling ratio Q (%) and the soluble fraction w_{sol} (%) are calculated according to the following equations:

$$Q (\%) = \frac{m_s - m_d}{m_d} \times 100$$
$$w_{\text{sol}} (\%) = \left(1 - \frac{m_d}{m_0}\right) \times 100$$

g. Tensile tests

Tensile tests were carried out using a QTest 25 machine from MTS Systems, equipped with a 500 N load cell. The deformation rate was set to $5 \text{ mm} \cdot \text{min}^{-1}$. For each polymer analyzed, four type 5B

specimens (ISO 527-2) were tested, with a thickness of approximately 1.8 mm, a width of ~2.0 mm, and an overall length of ~40 mm.

3. Synthesis of AGC

5CC was synthesized according to the synthesis protocol reported by Dannecker *et al.* for the synthesis of erythritol dicarbonate. 6.6 g of 3-allyloxy-1,2-propanediol (0.05 mol, 1 eq.), 120 mL of DMC (1.43 mol, ~30 eq.), and 0.35 g of TBD (0.0025 mol, 0.05 eq.) are introduced into a round-bottom flask. The flask is then fitted to a rotary evaporator, with the water bath preheated to 60 °C. The pressure is reduced to 314 mbar and the rotation set to 200 rpm. After 1 hour of reaction, the pressure is further reduced to evaporate the residual DMC. The crude product is then dissolved in 10 mL of dichloromethane, and several liquid-liquid extractions with 10 mL of water are performed in a separatory funnel. Extractions are carried out until the pH of the aqueous phase is neutral (monitored by pH paper). Typically, 4 to 6 successive extractions are necessary to remove the TBD. The organic phase is then dried with MgSO₄, filtered through cotton, and the dichloromethane is evaporated using the rotary evaporator. 5.56 g of pure **5CC** are recovered after purification (purification yield = 70%).

4. Synthesis tri-5CC and tetra-5CC

For all syntheses, the AUVcure UV chamber is used with a 10x10 cm LED source ($\lambda = 365$ nm) with an intensity of 1500 mW.cm⁻². The irradiations are done with the intensity set to 100%. A battery-powered AccuMix magnetic stirring plate is added to the chamber. 1 equivalent of the chosen thiol is introduced into a quartz flask and mixed with 3 (trithiol) or 4 (tetrathiol) equivalents of **5CC**. The volume of THF is calculated so that the concentration of reactive thiol and carbonate functions is [SH]=[CC]=0.75 mol.L⁻¹. 0.5 mol% (moles of reactive functions) of DMPA is added. The flask is then placed on a cork support on the stirring plate installed in the UV chamber and left open. The irradiations are initially done in 5-minute bursts to take a fraction of the reaction medium and analyze it by ¹H NMR, as well as to limit the temperature increase in the chamber. Once the necessary irradiation time is known for each synthesis, a stepwise irradiation program is set up with 5-minute irradiation steps interspersed with 3-minute non-irradiation steps.

5. Preparation of PHU thermosets

The carbonate is weighed in a cup, and the amount of diamine needed for crosslinking is measured with a micropipette, previously calibrated with the diamine, and placed next to the carbonate. In the case of solid 8DA, the diamine is first ground with a mortar and pestle. The mixture is then homogenized at t_0 with a spatula and poured into a silicone mold. Crosslinking then takes place in an oven thermostated at T = 25 °C for 24 hours.

6. In-situ monitoring of the PHU crosslinking reaction

a. Infrared monitoring

The reaction medium is prepared as described above. Immediately after homogenization, the mixture is quickly placed on the thermostated plate at $T = 25\text{ }^{\circ}\text{C}$ of the infrared spectrometer. Spectra are acquired every hour to monitor the conversion of carbonate functions during polymerization.

The conversion of carbonate functions was monitored by the decrease in the intensity of the $\nu_{\text{C=O}}$, 5CC . Thus, the intensity of this absorption band at a given time t , $A_{\text{carbonate}}^t$, is measured on the spectrum acquired at time t relative to a baseline. The intensity of the $\nu_{\text{C-H}}$ absorption band at 2920 cm^{-1} , $A_{\text{reference}}^t$, is used to calculate the normalized absorbances of the chemical functions of interest at time t , $\bar{A}_{\text{carbonate}}^t$, according to the equation:

$$\bar{A}_{\text{carbonate}}^t = \frac{A_{\text{carbonate}}^t}{A_{\text{reference}}^t}$$

The conversion of carbonate functions, $\alpha_{\text{carbonate}}$ (%), as a function of time (t) was then calculated according to the equation following the Beer-Lambert law:

$$\alpha_{\text{carbonate}} = \left(1 - \frac{\bar{A}_{\text{carbonate}}^t}{\bar{A}_{\text{carbonate}}^0} \right) \times 100$$

b. Rheology monitoring

After homogenizing the reactants, the mixture is placed in the 1 mm gap of the parallel-plate geometry ($\Phi = 8\text{ mm}$) and the oven is closed and thermostated at $T = 25\text{ }^{\circ}\text{C}$. The multifrequency mode is used for monitoring. A deformation amplitude of 1% at an angular velocity of $1\text{ rad}\cdot\text{s}^{-1}$ is applied to measure the elastic modulus G' and the viscous modulus G'' every 5 minutes for the following 5 frequencies: 1, 3, 6, 10, and $30\text{ rad}\cdot\text{s}^{-1}$.

The gel time, t_{gel} , corresponds to the moment when the Winter and Chambon criterion is met, *i.e.*, $G'(\omega) \sim G''(\omega) \sim \omega^n$. Thus, t_{gel} corresponds to the time (t) when the representative curves of (G') and (G'') as a function of ω are linear and parallel, on a logarithmic scale, with a slope equal to (n). The gel time can also be identified by plotting the loss factor $\tan(\delta) = G''/G'$ as a function of time. In this case, t_{gel} corresponds to the time (t) when all the representative curves of $\tan(\delta)$ coincide at a single point.

7. Calculation of the conversion at the gel point, α_{gel} , according to the Flory-Stockmayer theory

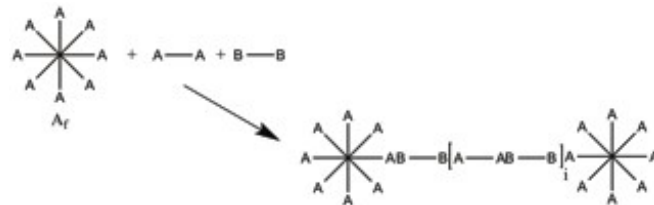
The theory of Flory-Stockmayer¹⁻³ describe the conversion of growing polymers to insoluble gels which occurs through crosslinking. This theory is a statistical approach assuming that polymers approach infinite size at the gel point, *i.e.* they become one gigantic molecule. It provides more accurate results than the Carother's approach, and it is applicable to systems with *non-stoichiometric ratios* of two or more different functional groups.

Flory-Stockmayer model is based on two assumptions: (1) the reactivity of all functional group of the same type is the same and independent of the molecular size, (2) there are no intramolecular reactions between functional group of the same molecule.

Typically, Flory and Stockmayer consider a system made of three types of monomer units (schematically represented in Scheme 1), where A reacts with B:

- Linear units with two A groups
- Linear units with two B groups
- Branched units with f A groups

These units are typically noted A_2 , B_2 and A_f , where f is the number of reactive functions on the branched unit.



Scheme 1

The central notion of the Flory-Stockmayer theory is the **branching probability**, α . It is the probability that a branch arising at a branch point leads *via* bifunctional unit to another branch point (rather than to a non-branch point or dead-end). Using an iterative approach, they demonstrated that, in order to obtain an infinite network (i.e. gelation), α must be strictly superior than a critical value, α_c , define as :

$$\alpha_c = \frac{1}{1-f}$$

where f is the functionality of the branch unit, *i.e.* the number of chain section meeting at the branch point, which, in turn, is the functionality of the monomer with functionality greater than 2, A_f . The quantity α_c is called the **critical branching coefficient** for gel formation. If more than one monomer with $f > 2$ is present, an average value of f is used. For example, for a system:

$$A_2 (x \text{ mol}), B_2 (y \text{ mol}), A_{f1} (z_1 \text{ mol}), A_{f2} (z_2 \text{ mol})$$

$$f = \frac{z_1 \cdot f_1 + z_2 \cdot f_2}{z_1 + z_2}$$

Going further into their statistical approach, Flory and Stockmayer were able to express the branching probability as a function of :

- p_A , the fraction of A group reacted (i.e. the conversion of A)
- ρ , the fraction of A group on all branched unit A_f
- r , the ratio of all A groups to all B groups

$$\alpha = \frac{rp_A^2\rho}{1-rp_A^2(1-\rho)}$$

At the gel point, $\alpha = \alpha_c = \frac{1}{1-f}$

Thus, one can calculate the conversion of function A at the gel point, p_A :

$$\frac{1}{1-f} = \frac{rp_A^2\rho}{1-rp_A^2(1-\rho)}$$

gives

$$p_A = \frac{1}{[r + r\rho(f-2)]^{1/2}}$$

The conversion at the gel point is usually noted p_c , the critical conversion:

$$p_c = \frac{1}{[r + r\rho(f-2)]^{1/2}}$$

For a given system, it is possible to obtain a gel or infinite network, if $0 < p_c < 1$.

Let's consider again the following system as an example:



In this case:

- $f = \frac{z_1 \cdot f_1 + z_2 \cdot f_2}{z_1 + z_2}$ (the average functionality of the unit with $f_x > 2$)
- $\rho = \frac{z_1 \cdot f_1 + z_2 \cdot f_2}{x \cdot 2 + z_1 \cdot f_1 + z_2 \cdot f_2}$
- $r = \frac{x \cdot 2 + z_1 \cdot f_1 + z_2 \cdot f_2}{y \cdot 2}$

If we now consider the system tri-5CC + tetra-5CC + tDA:

75	25	3.25	67
50	50	3.5	63
25	75	3.75	60
0	100	4	58

II. Supplementary data

1. NMR, FTIR and MS characterizations of AGC

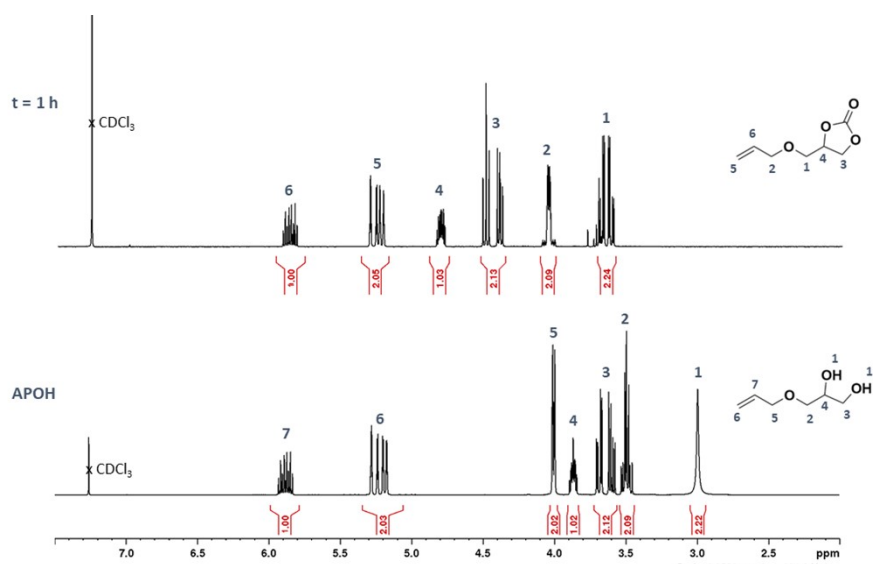


Figure S1 : ¹H NMR spectrum of the crude after 1h of reaction for the synthesis of AGC, as compared to the ¹H NMR spectrum of the starting diol

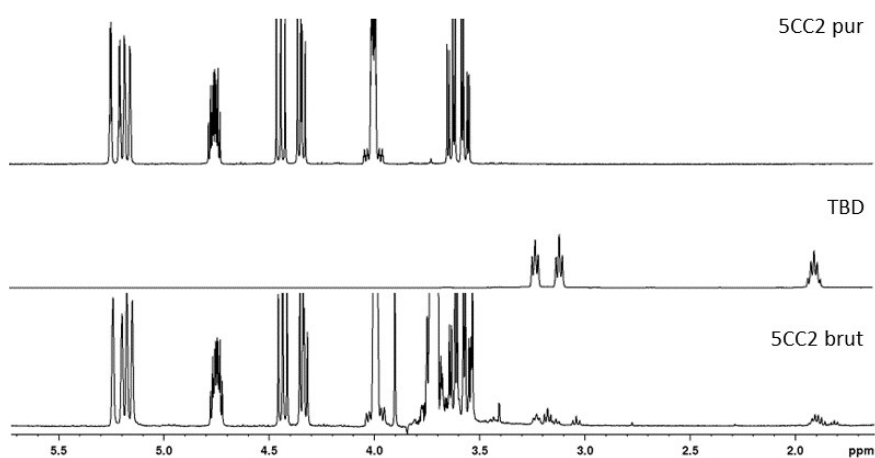


Figure S2 : ^1H NMR spectrum of AGC after purification as compared to the ^1H NMR spectra of TBD and the crude after 1h of reaction (CDCl_3)

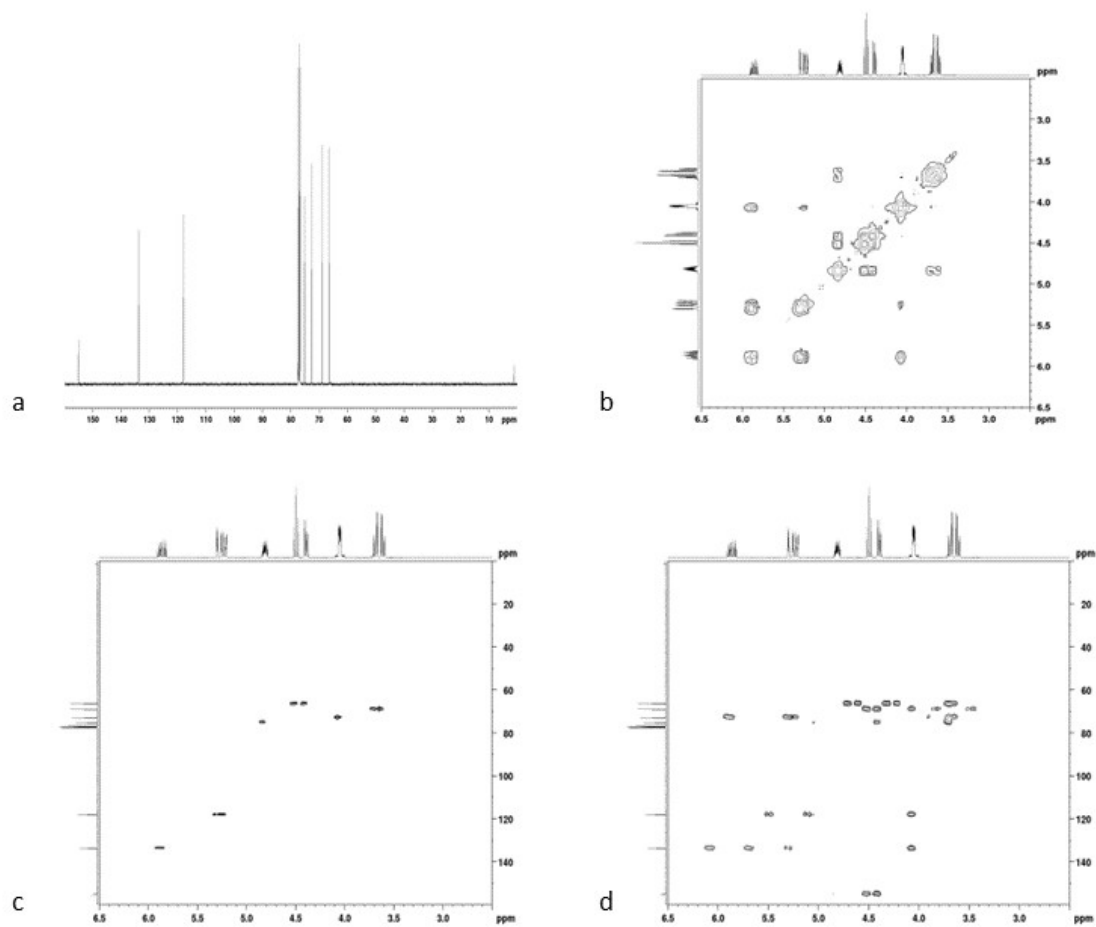


Figure S3 : NMR characterizations of AGC in CDCl_3 : (a) ^{13}C ; (b) COSY ; (c) HSQC ; (d) HMBC

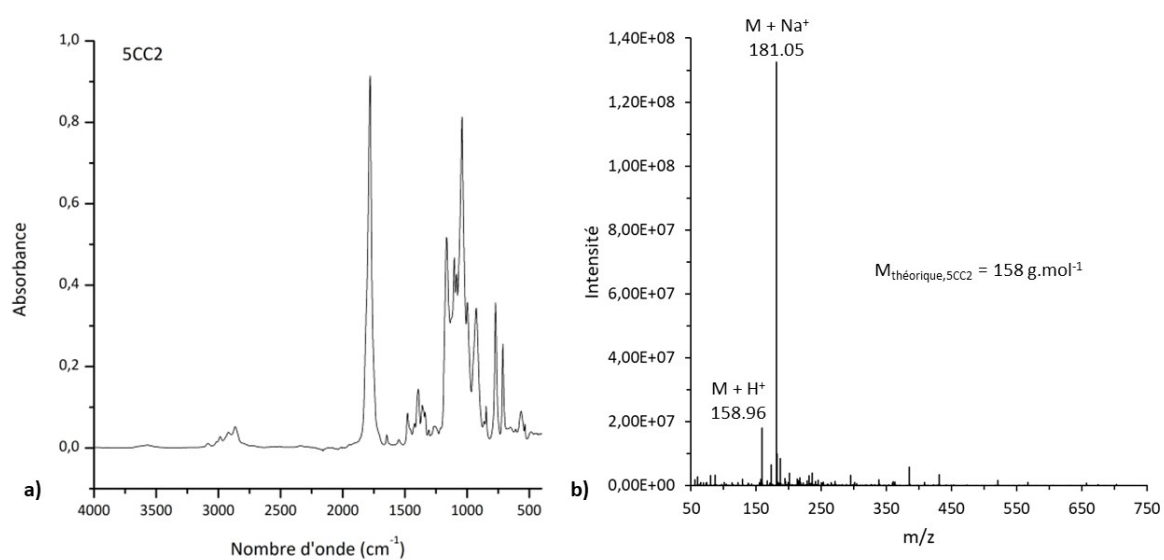


Figure S4 : (a) FTIR and (b) mass (acetonitrile, 1 mg ml^{-1}) spectra of AGC

2. Kinetics for the synthesis of tri-5CC and tetra-5CC

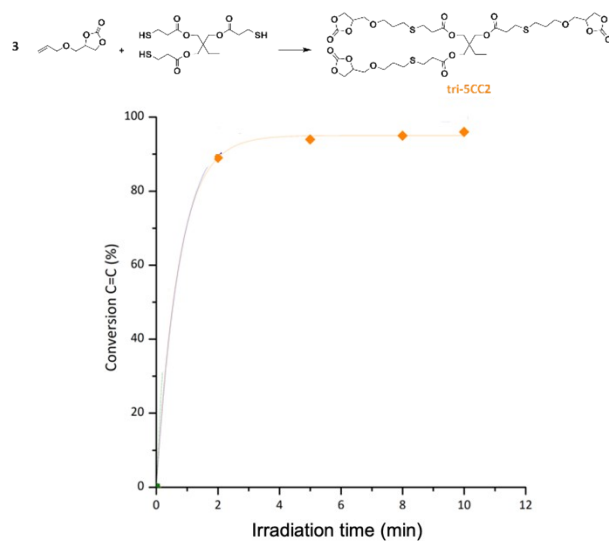


Figure S5 : Allyl (C=C) conversion as a function of time for the synthesis of tri-5CC in THF (0.75 mol L⁻¹, DMPA 0.5 mol%, $\lambda = 365$ nm) as measured by ¹H NMR spectroscopy.

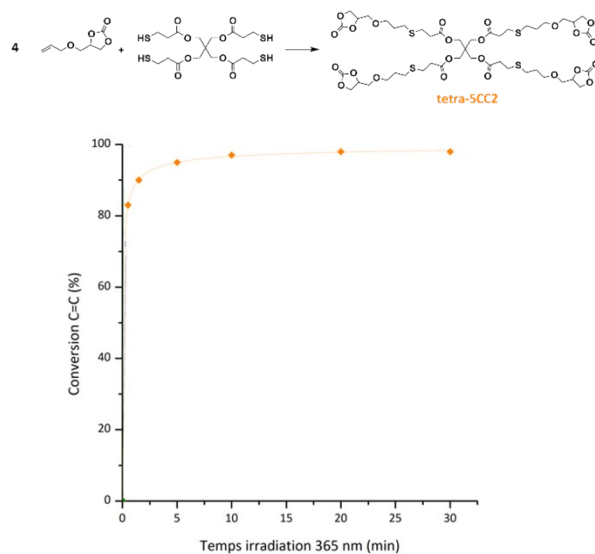


Figure S6 : Allyl (C=C) conversion as a function of time for the synthesis of tetra-5CC in THF (0.75 mol L⁻¹, DMPA 0.5 mol%, $\lambda = 365$ nm) as measured by ¹H NMR spectroscopy.

3. NMR, FTIR and MS characterizations of tri-5CC

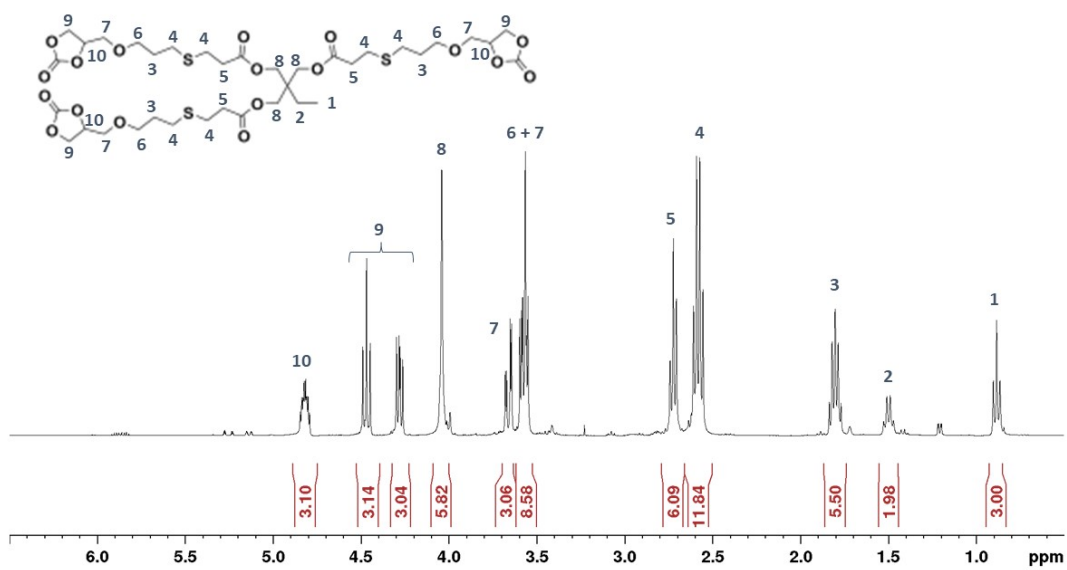


Figure S7 : ^1H NMR spectrum of tri-5CC in THF-d_8

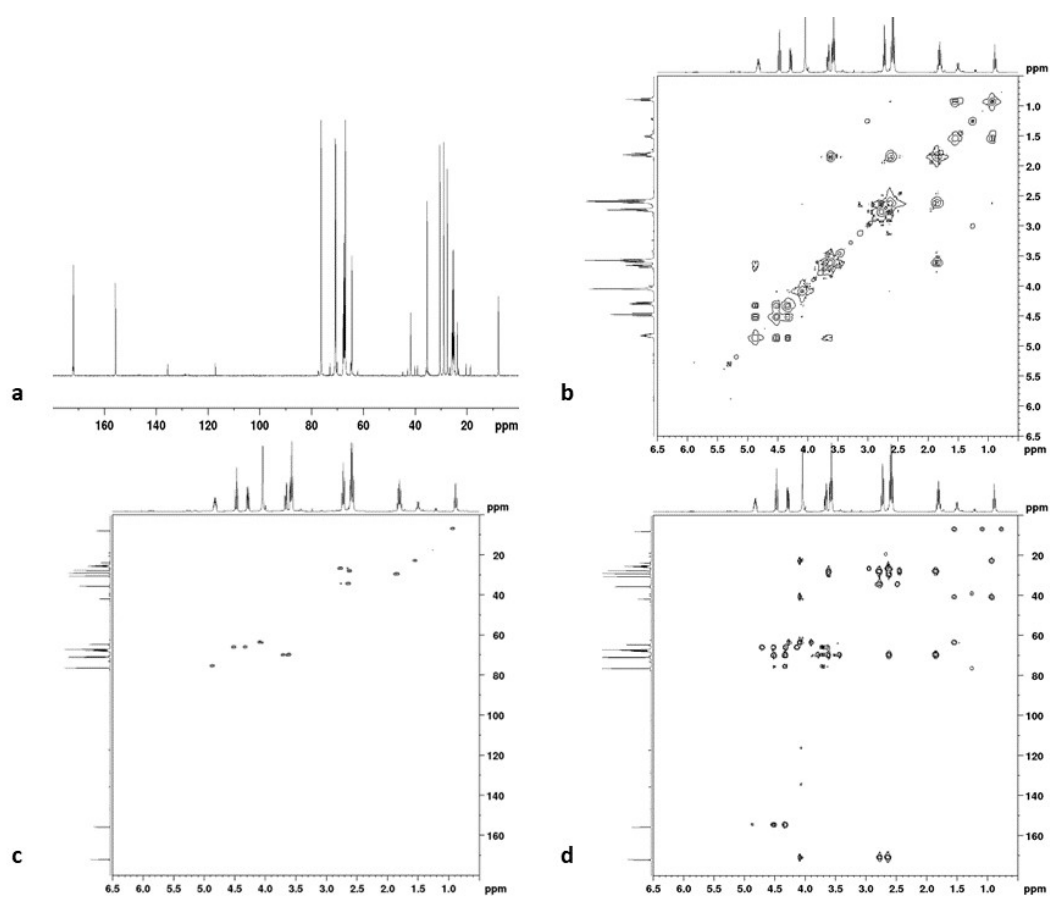


Figure S8 : NMR characterizations of tri-5CC in THF-d_8 : (a) ^{13}C ; (b) COSY ; (c) HSQC ; (d) HMBC

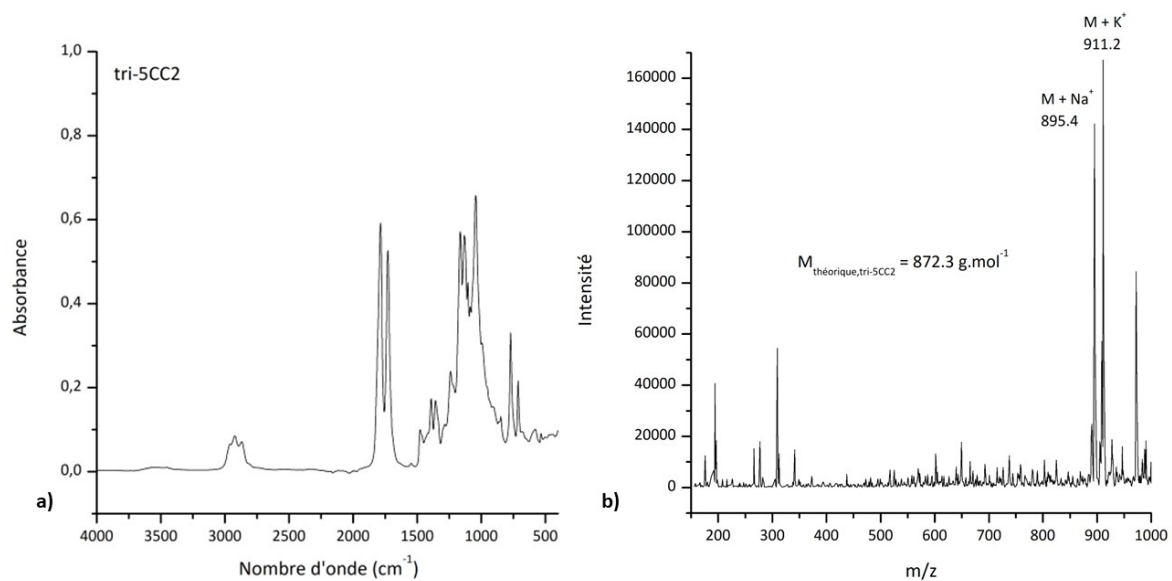


Figure S9 : (a) FTIR and (b) mass (acetonitrile, 1 mg ml⁻¹) spectra of tri-5CC

4. NMR, FTIR and MS characterizations of tetra-5CC

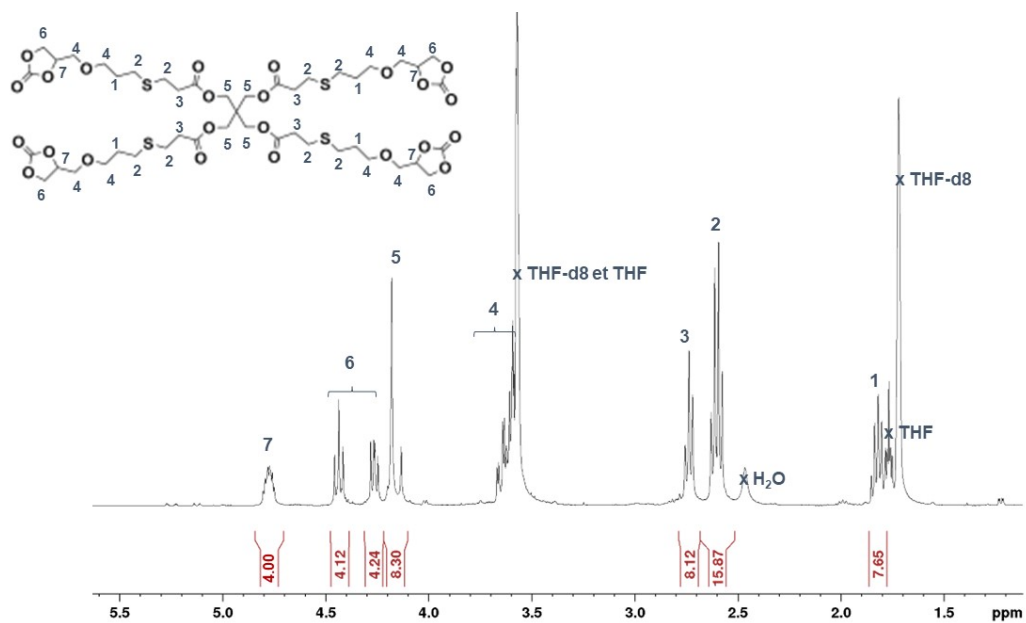


Figure S10 : ¹H NMR spectrum of tetra-5CC in THF-d₈

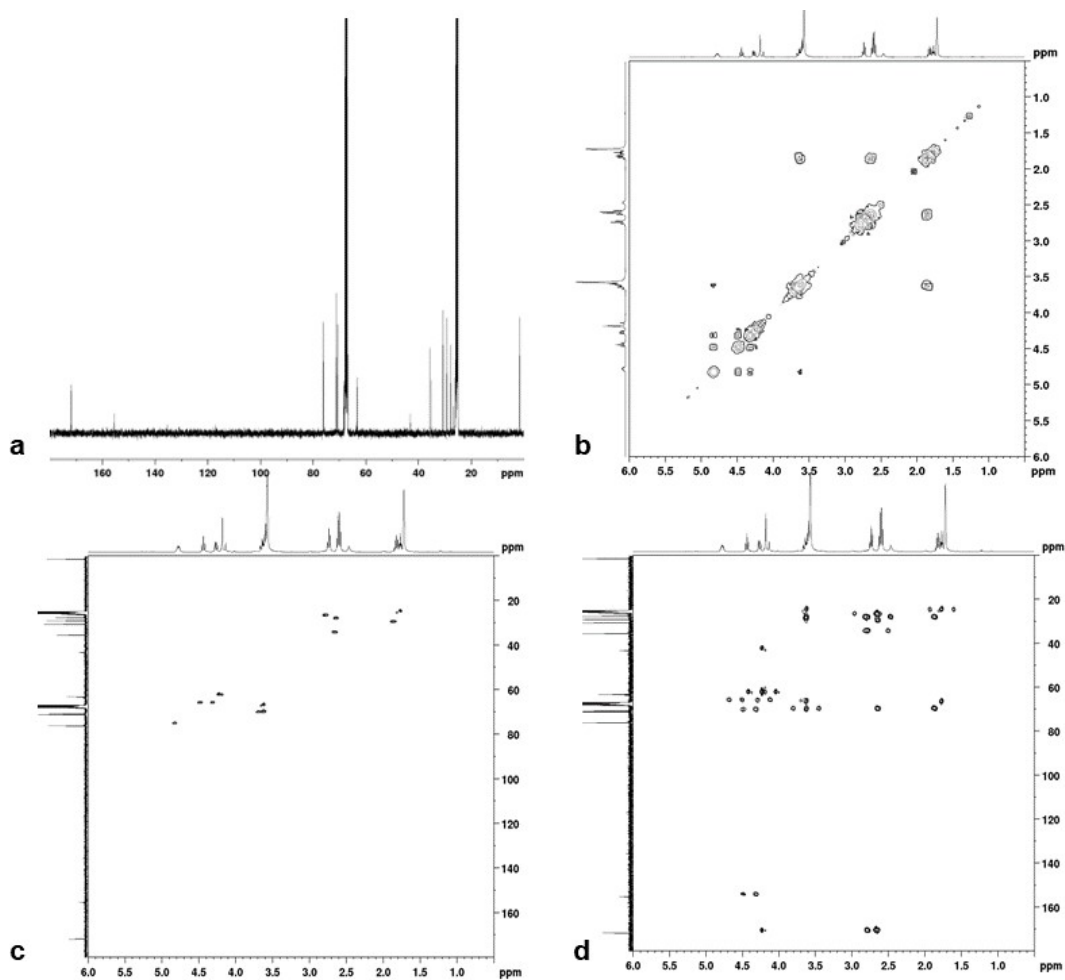


Figure S11 : NMR characterizations of tetra-5CC in THF-d₈ : (a) ¹³C ; (b) COSY ; (c) HSQC ; (d) HMBC

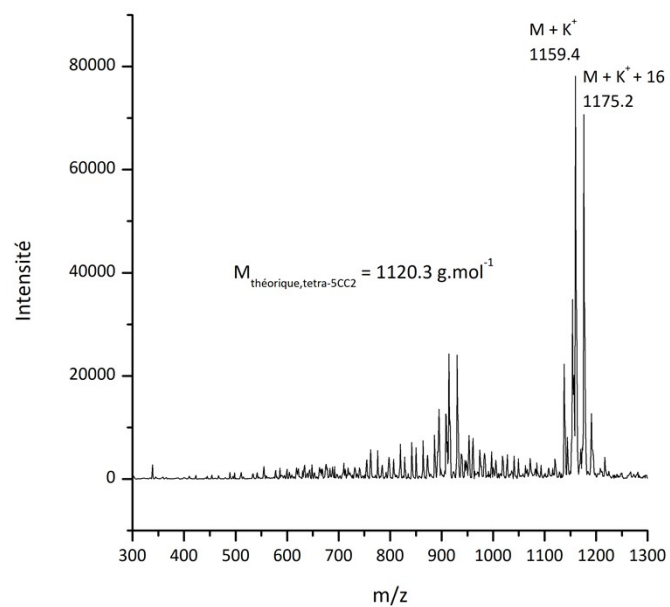


Figure S12 : mass (acetonitrile, 1 mg ml⁻¹) spectra of tetra-5CC

5. FTIR spectra of P1 to P6 (amine screening at RT)

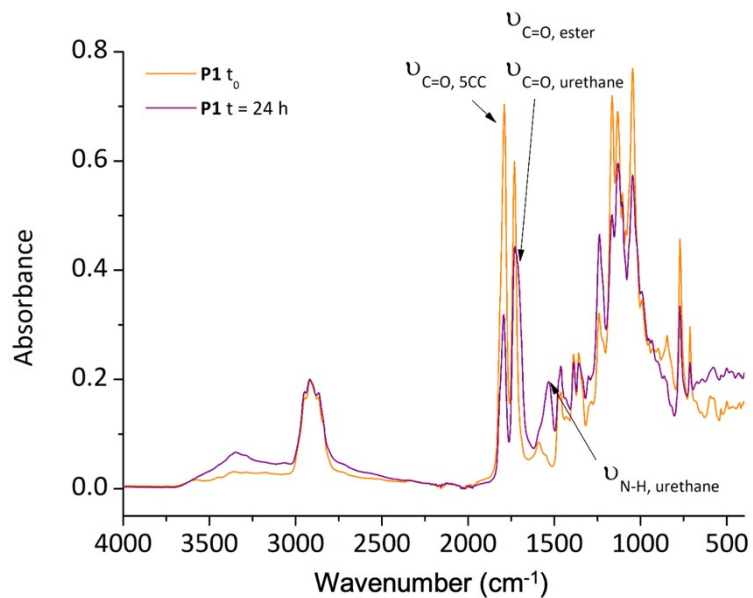


Figure S13 : Superimposition of the FTIR spectra of P1 (tri-5CC+IPDA) at t = 0 and after t = 24 h of crosslinking at RT

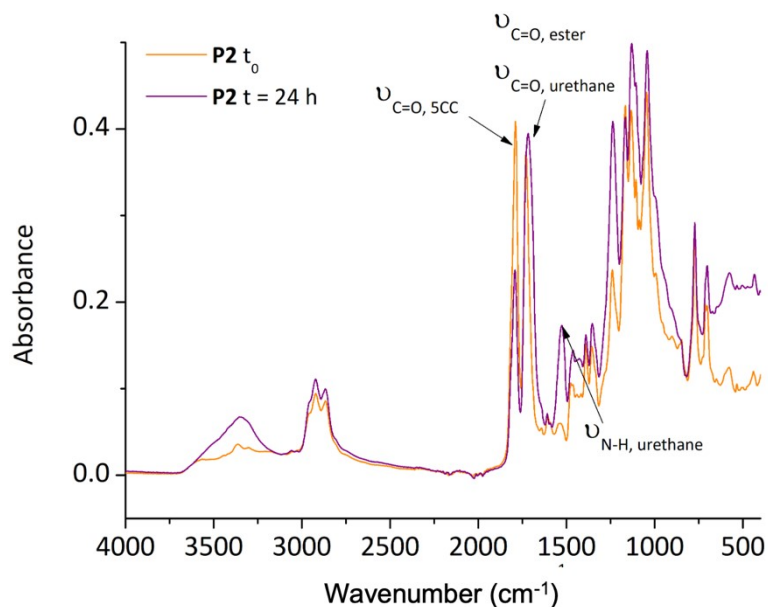


Figure S14 : Superimposition of the FTIR spectra of P2 (tri-5CC+mXDA) at t = 0 and after t = 24 h of crosslinking at RT

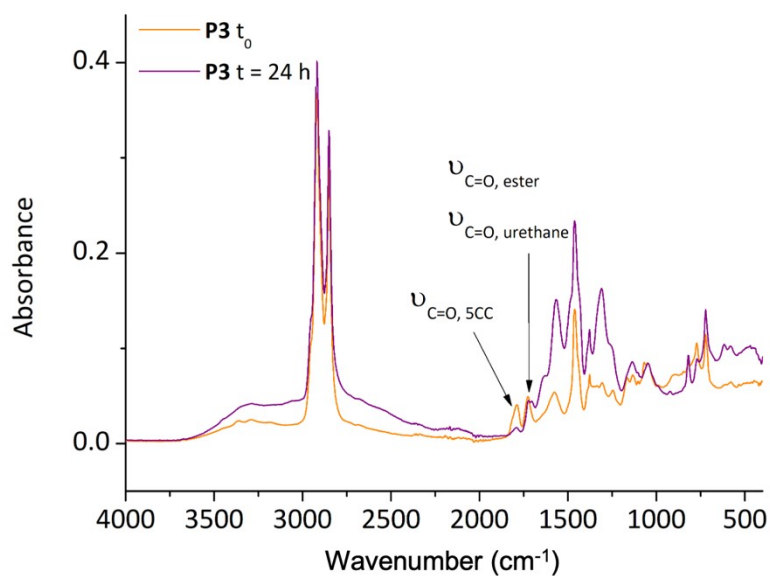


Figure S15 : Superimposition of the FTIR spectra of P3 (tri-5CC+Priamimne 1075) at $t = 0$ and after $t = 24$ h of crosslinking at RT

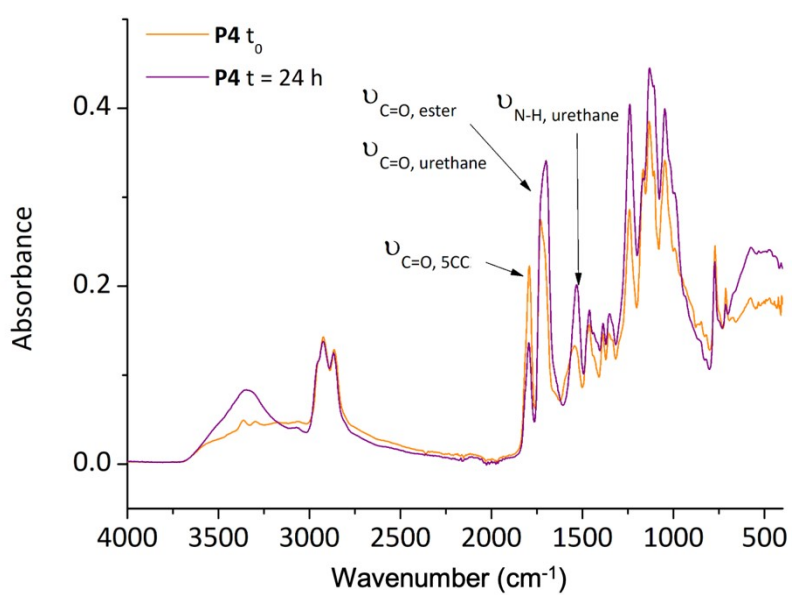


Figure S16 : Superimposition of the FTIR spectra of P4 (tri-5CC+2MDPA) at $t = 0$ and after $t = 24$ h of crosslinking at RT

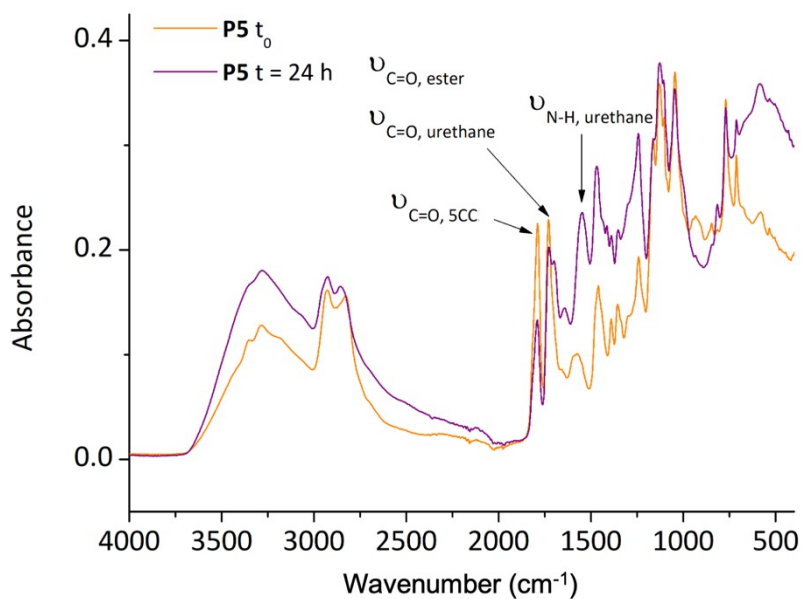


Figure S17 : Superimposition of the FTIR spectra of P5 (tri-5CC+TEPA) at $t = 0$ and after $t = 24$ h of crosslinking at RT

6. SEC analysis of the soluble fraction for the thermosets P1 to P6

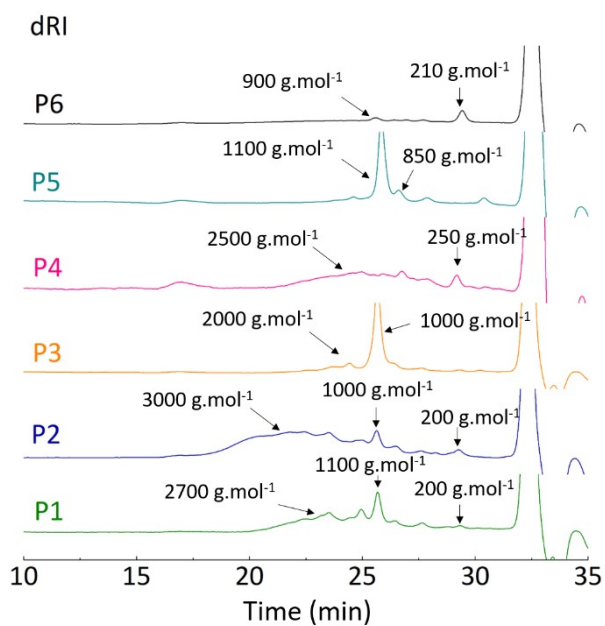


Figure S18 : SEC chromatograms (in THF) of the soluble fractions of thermosets P1, P2, P3, P4, P5 and P6 after crosslinking for 24 hours at room temperature

7. In-situ FTIR monitoring for the crosslinking reaction of P7 to P10

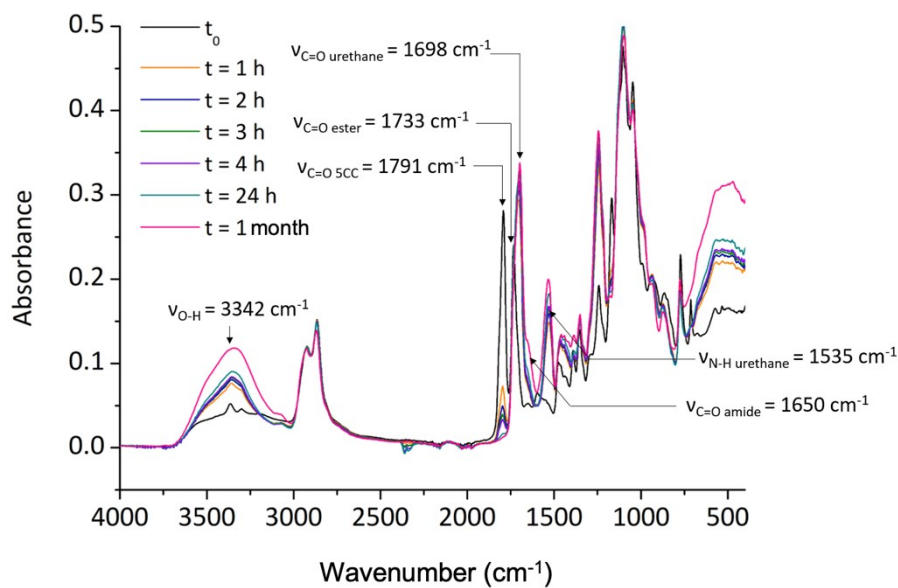


Figure S19 : Superimposition of the FTIR spectra of P7 (tri-5CC 75mol% +tetra-5CC 25mol% + tDA, X = 25) recorded at different time during crosslinking at RT

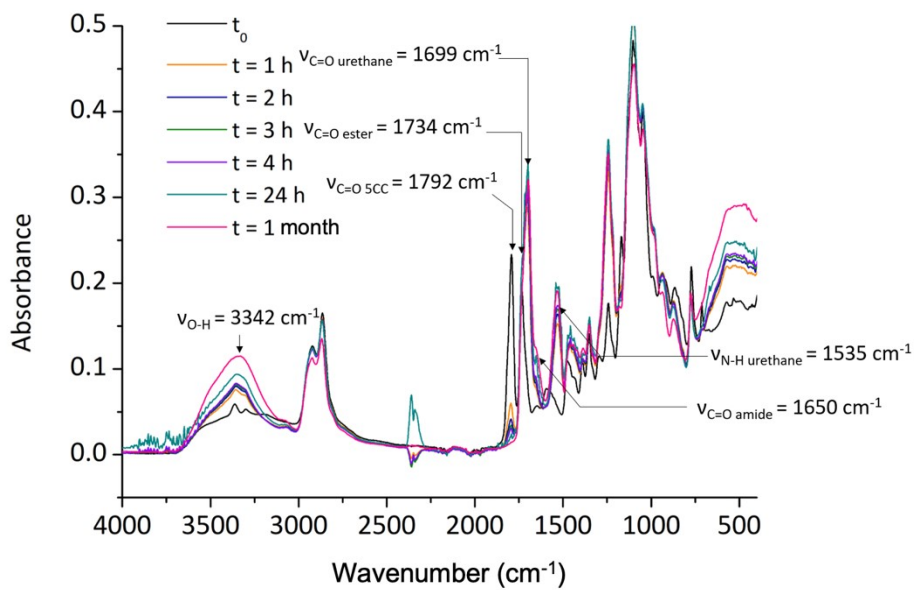


Figure S20 : Superimposition of the FTIR spectra of P8 (tri-5CC 50mol% +tetra-5CC 50mol% + tDA, X = 50) recorded at different time during crosslinking at RT

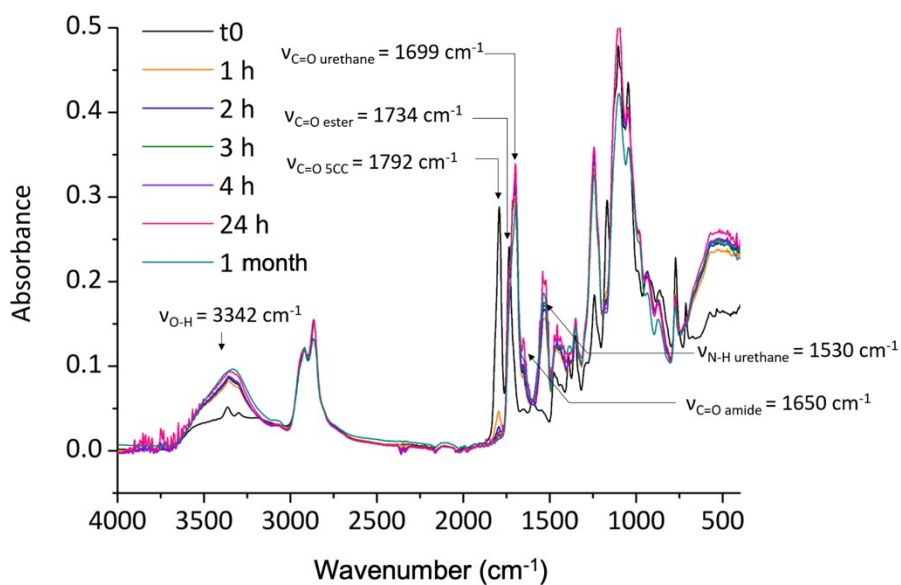


Figure S21 : Superimposition of the FTIR spectra of P9 (tri-5CC 25mol% + tetra-5CC 75mol% + tDA, X = 75) recorded at different time during crosslinking at RT

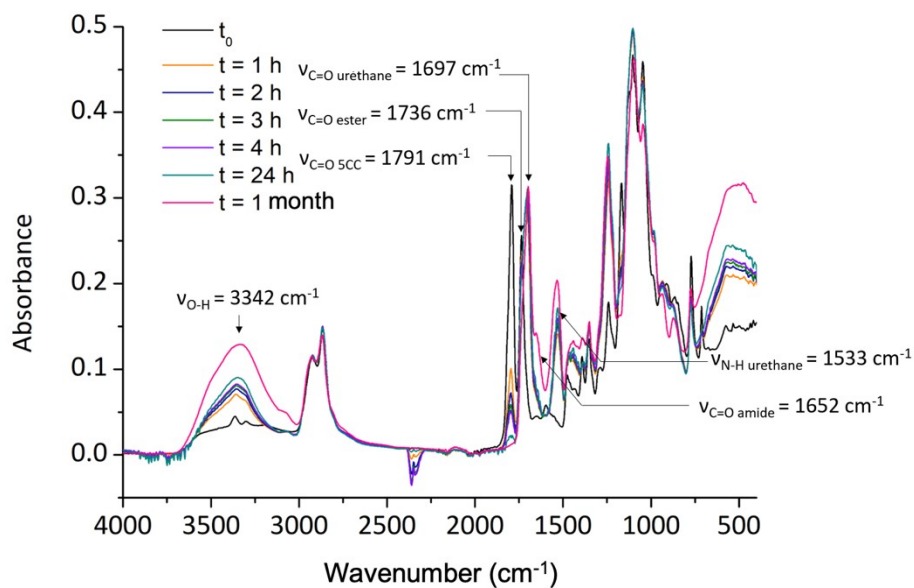


Figure S22 : Superimposition of the FTIR spectra of P10 (tetra-5CC + tDA, X = 100) recorded at different time during crosslinking at RT

8. In-situ rheology monitoring for the crosslinking reaction of P7 to P10

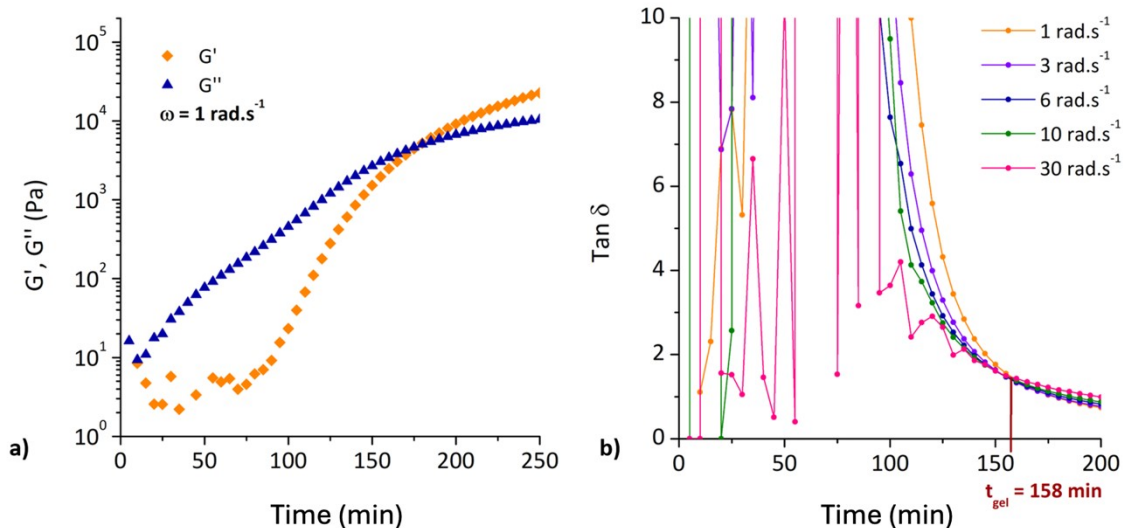


Figure S23 : In-situ rheology monitoring of the crosslinking reaction of **P7** (tri-5CC 75mol% +tetra-5CC 25mol% + tDA, X = 25) : **a**) Variation of the storage ($G'(\omega)$) and the loss ($G''(\omega)$) moduli as a function of time for $\omega = 1 \text{ rad.s}^{-1}$, and **b**) variation of the loss factor ($\tan(\delta)$) as a function of time for $\omega = 1, 3, 6, 10,$ and 30 rad.s^{-1} .

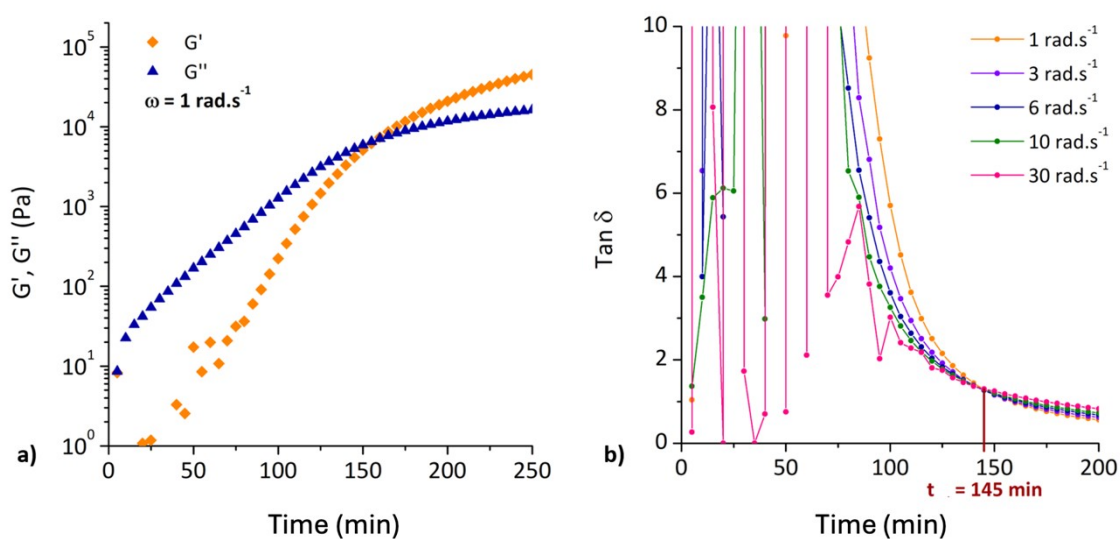


Figure S24 : In-situ rheology monitoring of the crosslinking reaction of **P8** (tri-5CC 50mol% +tetra-5CC 50mol% + tDA, X = 50) : **a**) Variation of the storage ($G'(\omega)$) and the loss ($G''(\omega)$) moduli as a function of time for $\omega = 1 \text{ rad.s}^{-1}$, and **b**) variation of the loss factor ($\tan(\delta)$) as a function of time for $\omega = 1, 3, 6, 10,$ and 30 rad.s^{-1} .

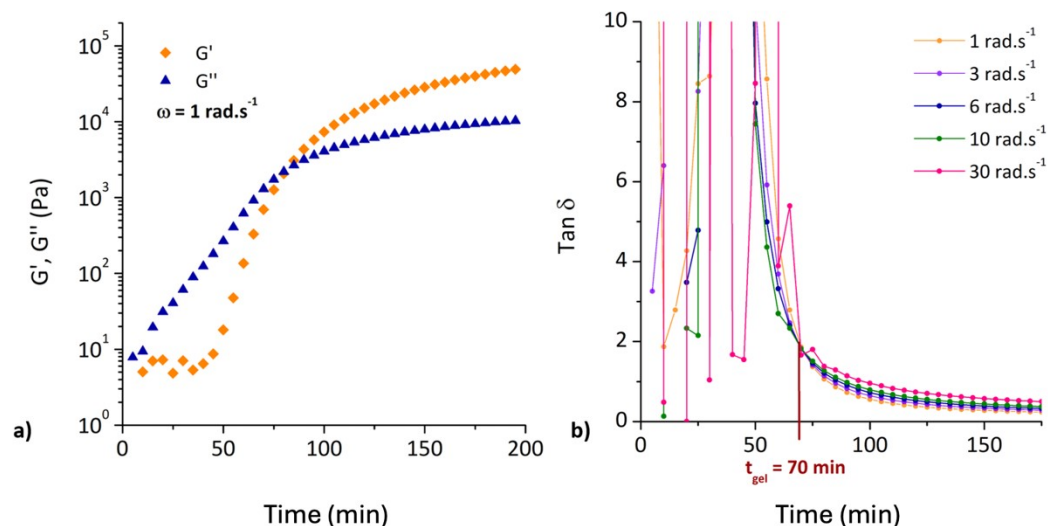


Figure S25 : In-situ rheology monitoring of the crosslinking reaction of **P9** (tri-5CC 25mol% +tetra-5CC 75mol% + tDA, X = 75) : **a)** Variation of the storage ($G'(\omega)$) and the loss ($G''(\omega)$) moduli as a function of time for $\omega = 1 \text{ rad.s}^{-1}$, and **b)** variation of the loss factor ($\tan(\delta)$) as a function of time for $\omega = 1, 3, 6, 10,$ and 30 rad.s^{-1} .

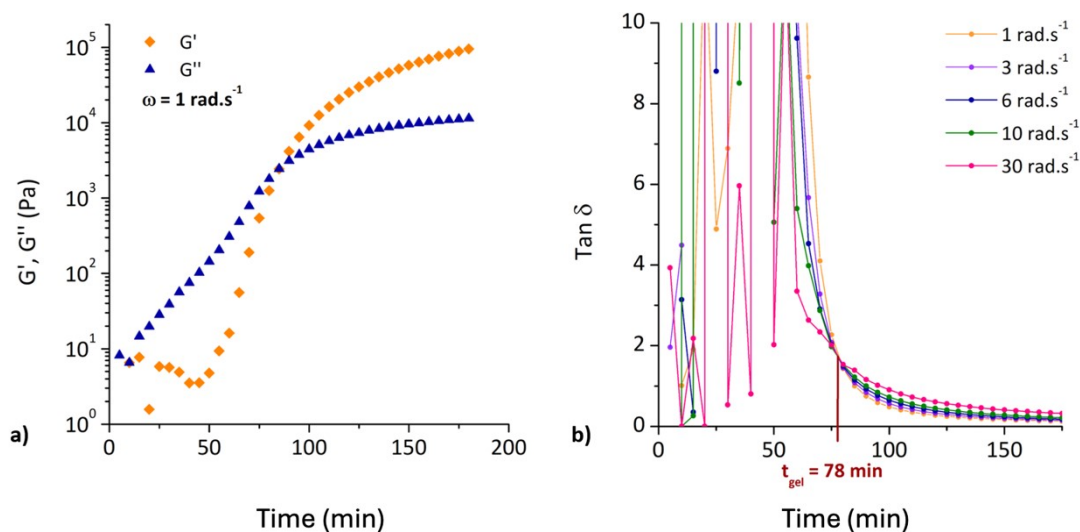


Figure S26 : In-situ rheology monitoring of the crosslinking reaction of **P10** (tetra-5CC + tDA, X = 100) : **a)** Variation of the storage ($G'(\omega)$) and the loss ($G''(\omega)$) moduli as a function of time for $\omega = 1 \text{ rad.s}^{-1}$, and **b)** variation of the loss factor ($\tan(\delta)$) as a function of time for $\omega = 1, 3, 6, 10,$ and 30 rad.s^{-1} .

9. SEC analysis of the soluble fraction for the thermosets P6 to P10

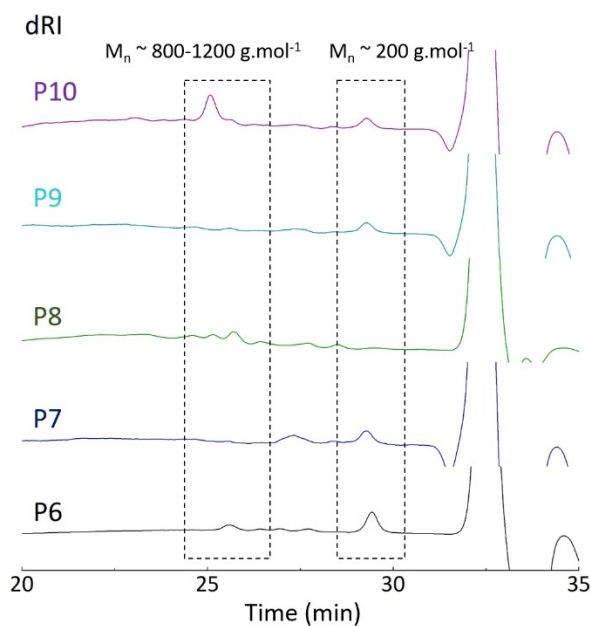


Figure S27 : SEC chromatograms (in THF) of the soluble fractions of thermosets P6, P7, P8, P9, and P10 after crosslinking for 24 hours at room temperature

10. DSC characterization of P8 after drying at 40 °C under vacuum

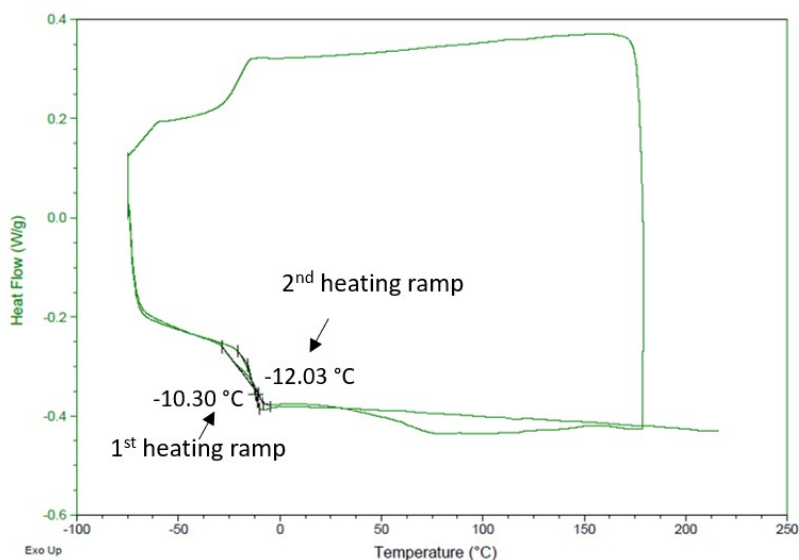


Figure S28 : DSC thermogram of P8 after 1 night drying under vacuum at 40 °C

Figure S28 shows the thermogram of dried P8. The T_g values of the first and second heating ramps are very similar, with $T_{g1} = -10 \text{ }^\circ\text{C}$ and $T_{g2} = -12 \text{ }^\circ\text{C}$. Furthermore, the intensity of the endothermic peak of the first heating ramp has significantly decreased, suggesting that the water was effectively removed

during the preliminary drying step. The T_g of the polymer dried at low temperature is very similar to that of the polymer heated above 180°C after the first heating cycle, indicating that the networks do not undergo significant post-crosslinking at high temperature. Thus, the difference between T_{g1} and T_{g2} for undried polymers is mainly due to the plasticizing effect of water.

11. DSC characterization of the thermosets P6 to P10

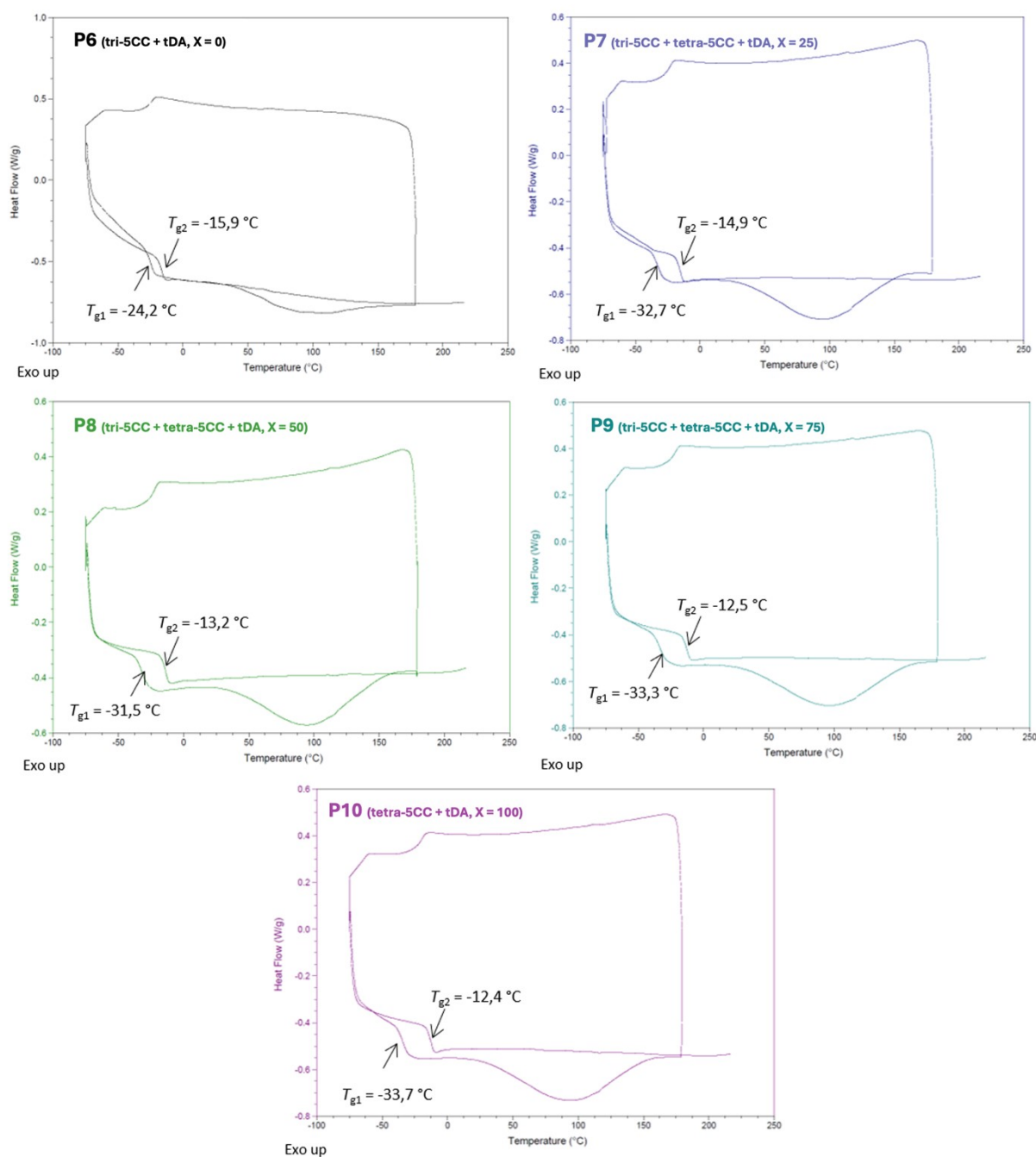


Figure S29 : DSC thermograms ($10\text{ }^{\circ}\text{C}\cdot\text{min}^{-1}$) of the thermosets P6, P7, P8, P9, and P10 crosslinked for 24 hours at room temperature

12. Stress – strain profiles for all the tested specimens of P6 to P10

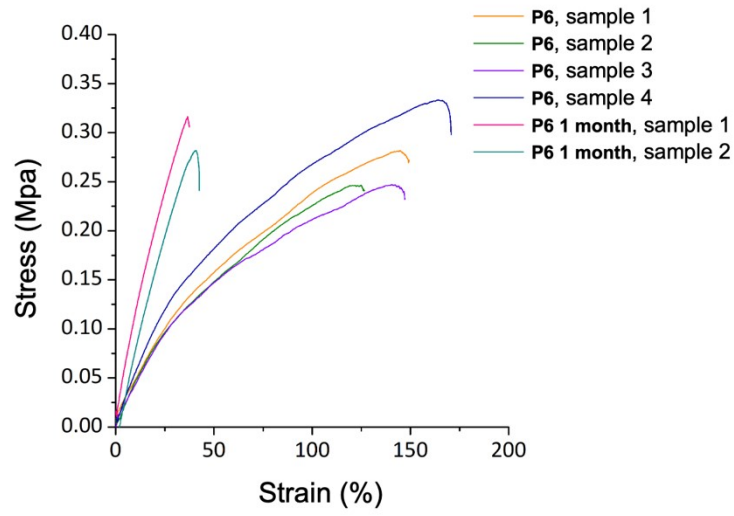


Figure S30 : Stress-strain tensile profiles for all the tested specimens of P6

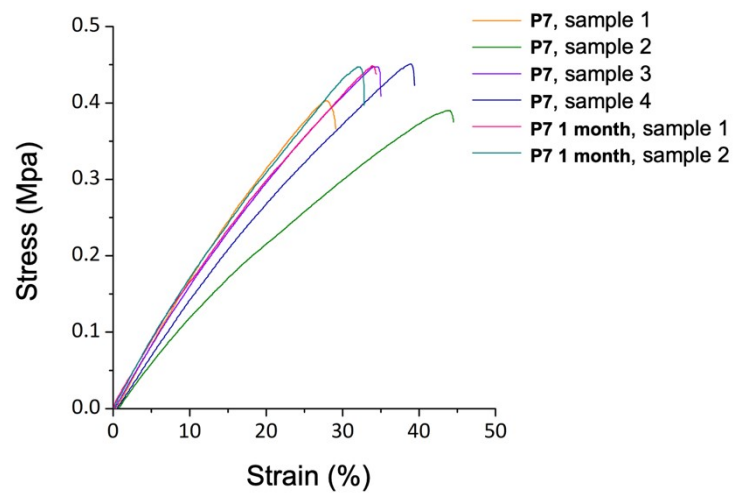


Figure S31 : Stress-strain tensile profiles for all the tested specimens of P7

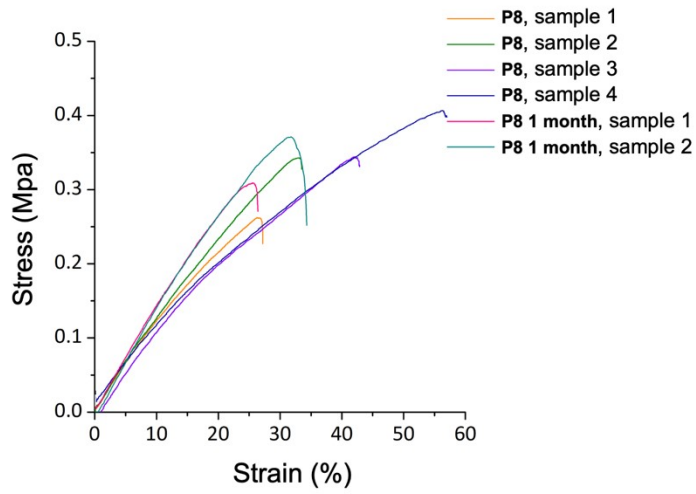


Figure S32 : Stress-strain tensile profiles for all the tested specimens of P8

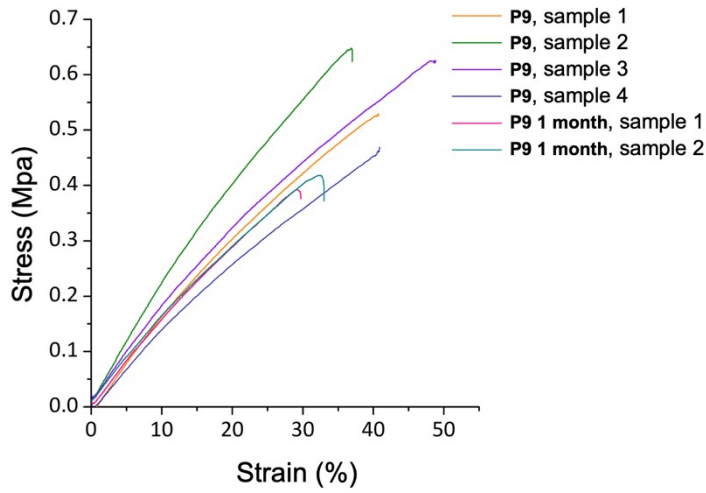


Figure S33 : Stress-strain tensile profiles for all the tested specimens of P9

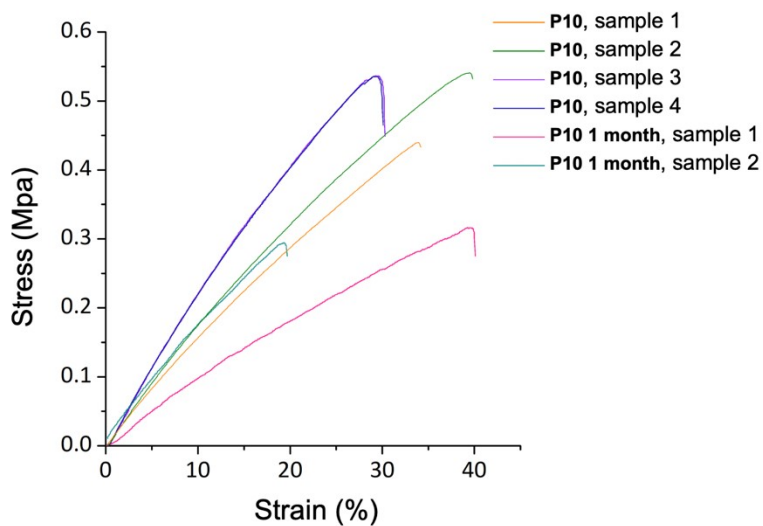


Figure S34 : Stress-strain tensile profiles for all the tested specimens of P10

13. FTIR spectra after 1-month storage for P6 to P10

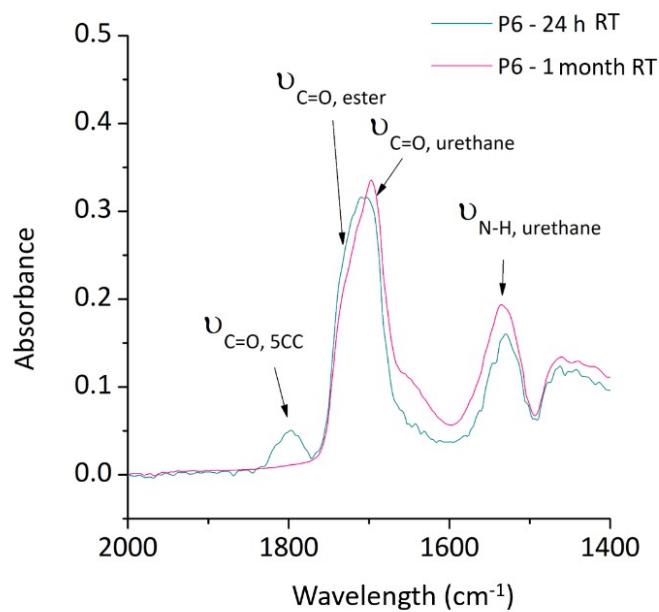


Figure S35 : Infrared spectra of P6 after 24 h and 1 month at room temperature

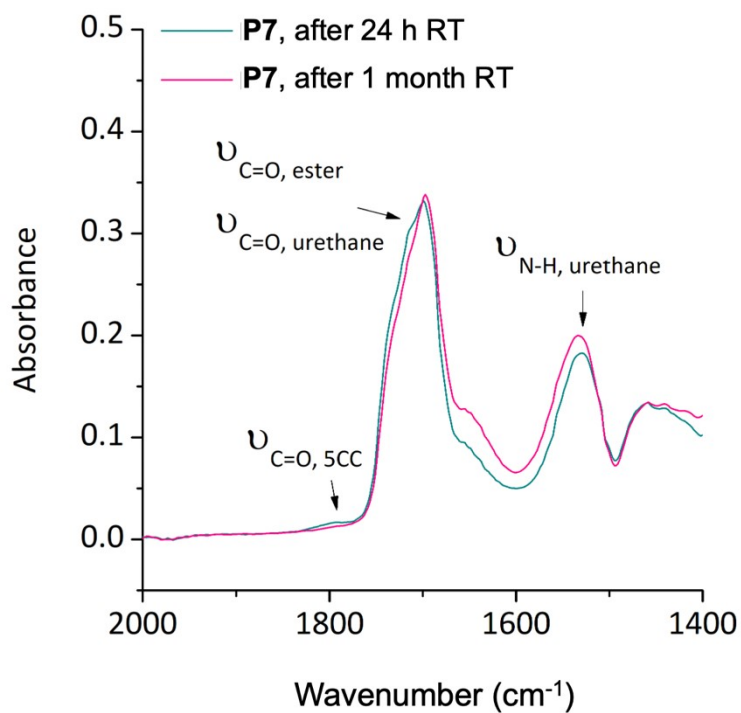


Figure S36 : Infrared spectra of P7 after 24 h and 1 month at room temperature

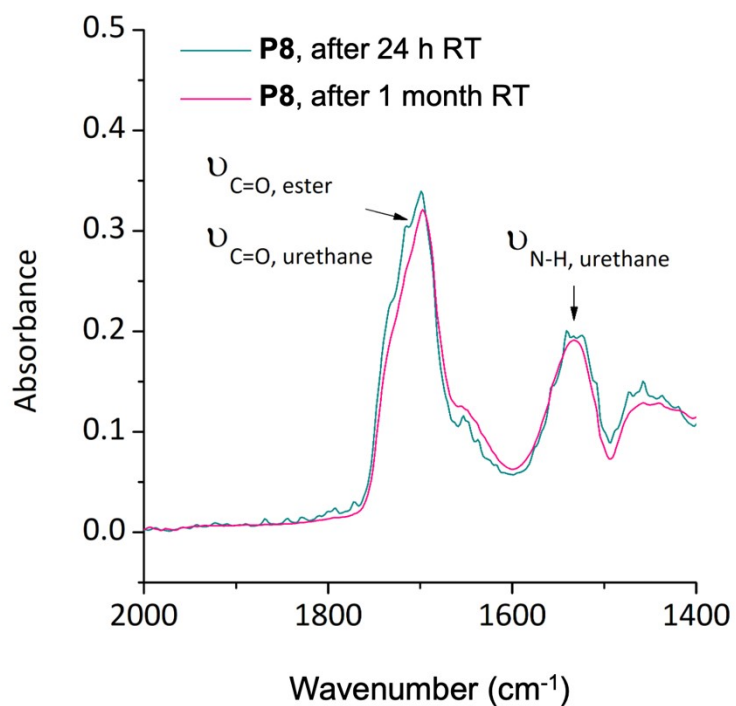


Figure S37 : Infrared spectra of P8 after 24 h and 1 month at room temperature

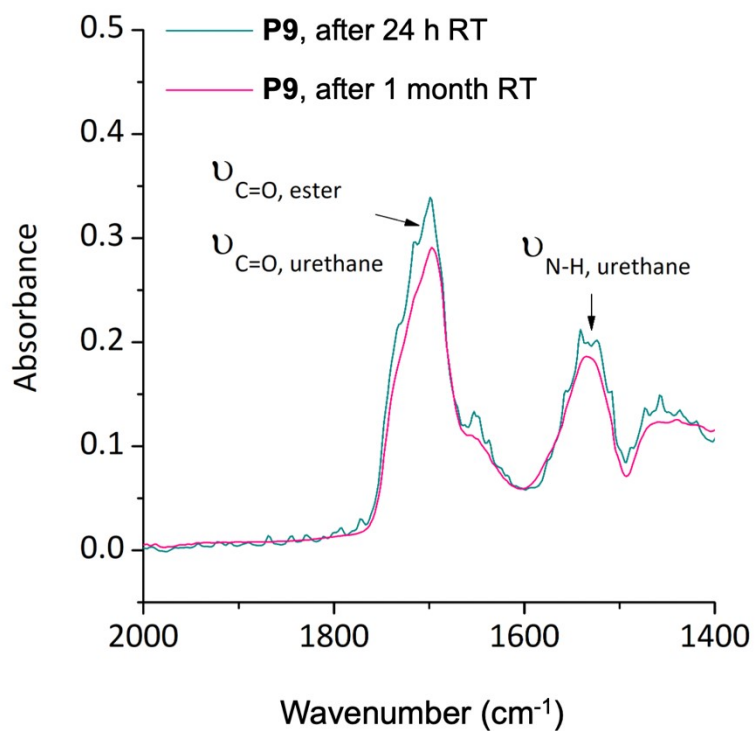


Figure S38 : Infrared spectra of P9 after 24 h and 1 month at room temperature

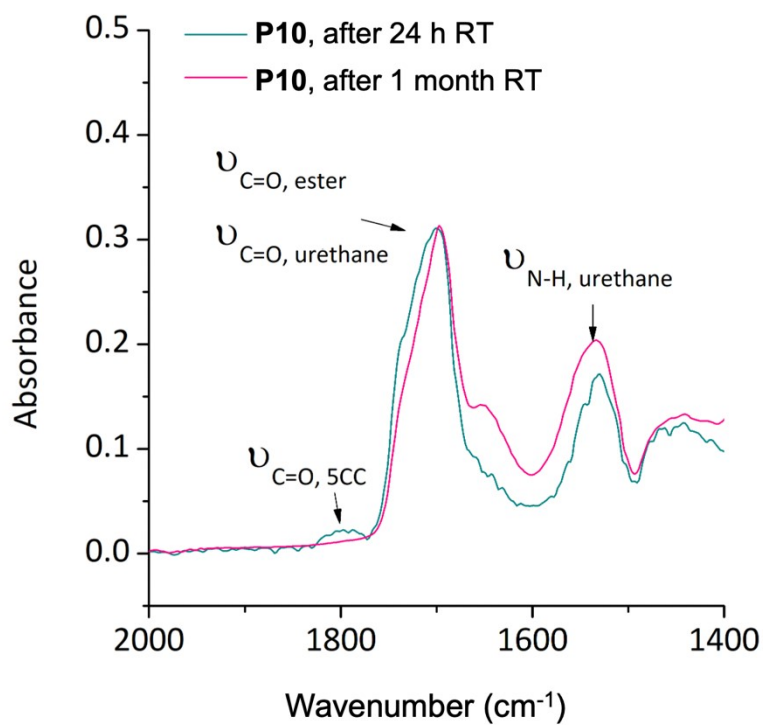


Figure S39 : Infrared spectra of P10 after 24 h and 1 month at room temperature

14. DSC thermograms after 1-month storage for P6 to P10

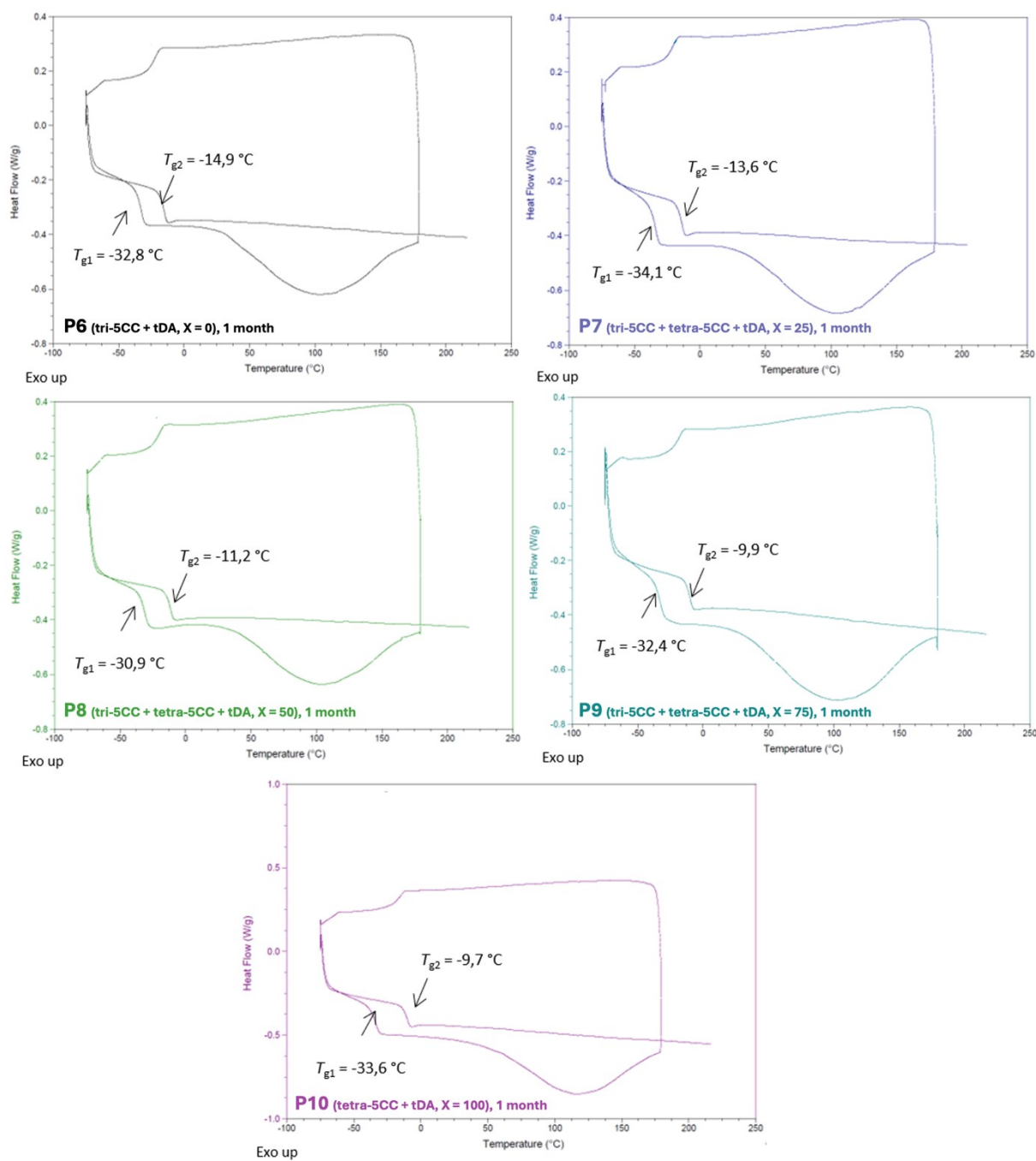


Figure S40 : DSC thermograms of P6, P7, P8, P9 and P10 after 1 month at room temperature

15. FTIR analysis of the tri-5CC + tDA system crosslinked at RT under inert atmosphere

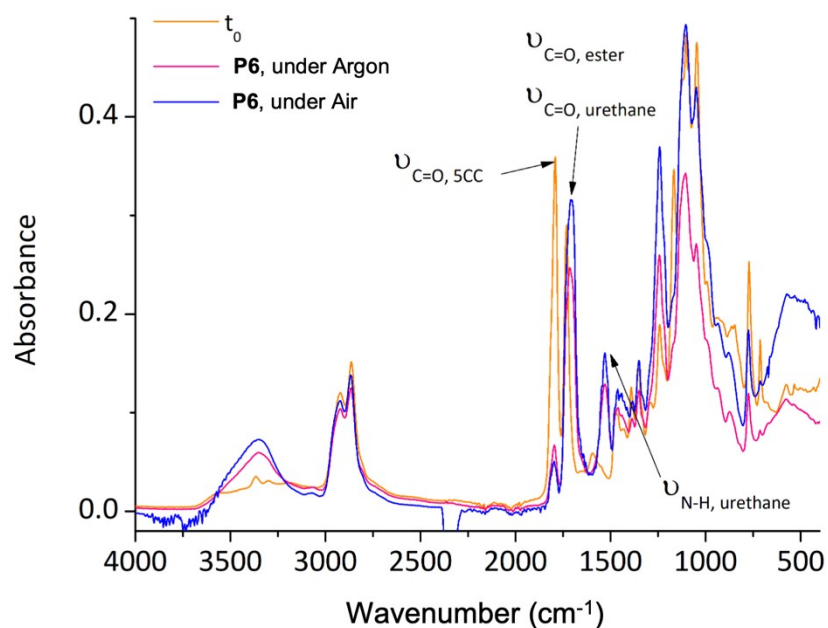


Figure S41 : Infrared spectra of P6 ($X = 0$ mol%) cured under air versus inert atmosphere (Argon)

16. SEC analysis of the sol fraction of the tri-5CC + tDA system crosslinked at RT under inert atmosphere

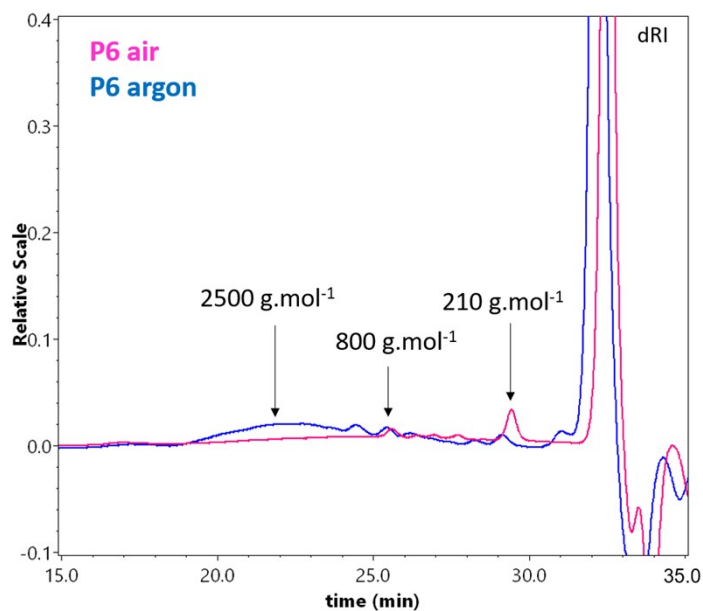


Figure S42 : SEC chromatograms of the soluble fraction of P6 ($X = 0$ mol%) cured under air versus inert atmosphere (Argon)

III. References

- (1) Flory, P. J. Molecular size distribution in three dimensional polymers. I. Gelation. *Journal of the American Chemical Society* **1941**, *63*, 3083-3090. DOI: 10.1021/ja01856a061.
- (2) Flory, P. J. Constitution of three-dimensional polymers and the theory of gelation. *Journal of Physical Chemistry* **1942**, *46* (1), 132-140, Article. DOI: 10.1021/j150415a016.
- (3) Stockmayer, W. H. Theory of molecular size distribution and gel formation in branched polymers II General cross linking. *Journal of Chemical Physics* **1944**, *12* (4), 125-131. DOI: 10.1063/1.1723922.